Article

Chemistry & Biology

Disarming *Pseudomonas aeruginosa* Virulence Factor LasB by Leveraging a *Caenorhabditis elegans* Infection Model

Graphical Abstract

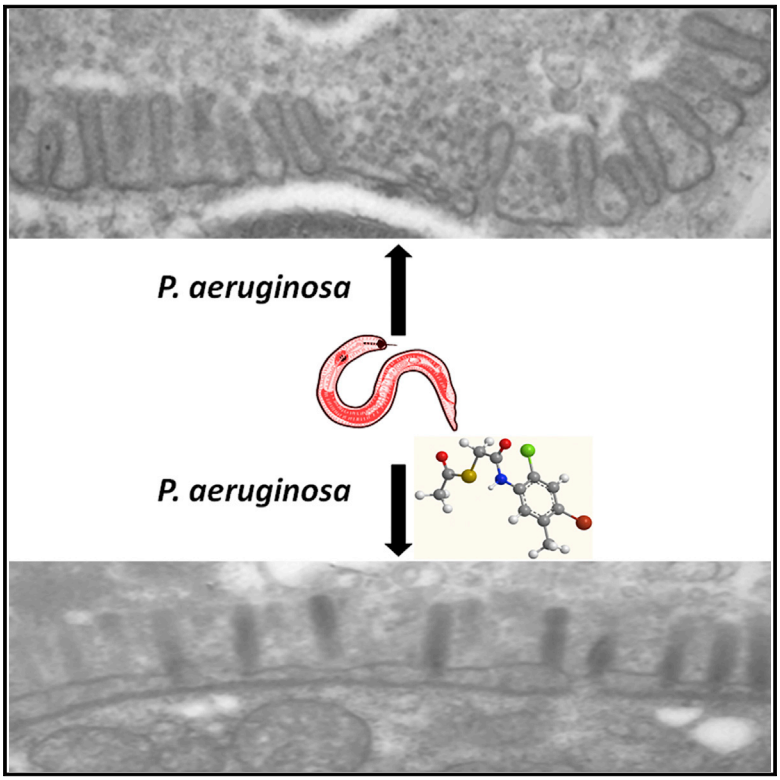

Authors

Jie Zhu, Xiaoqing Cai, ...,
Matthew Lardy, Kim D. Janda

Correspondence

kdjanda@scripps.edu

In Brief

Targeting virulence factors although challenging, offers tremendous potential for antibacterial therapeutics. Zhu et al. established a *C. elegans* infection model to study *P. aeruginosa* pathogenesis, which inspired the identification of molecules that could ablate LasB activity in this non-mammalian model organism.

Highlights

- A LasB inhibitor motif was identified using computational modeling
- *C. elegans* virulence factor infection model
- LasB knockout strain attenuated virulence in *C. elegans*
- Visualization of LasB virulence in *C. elegans* through TEM

Zhu et al., 2015, Chemistry & Biology *22*, 483–491
April 23, 2015 ©2015 Elsevier Ltd All rights reserved
http://dx.doi.org/10.1016/j.chembiol.2015.03.012

CellPress

Chemistry & Biology
Article

Disarming *Pseudomonas aeruginosa* Virulence Factor LasB by Leveraging a *Caenorhabditis elegans* Infection Model

Jie Zhu,[1] Xiaoqing Cai,[1] Tyler L. Harris,[1] Major Gooyit,[1] Malcolm Wood,[2] Matthew Lardy,[3] and Kim D. Janda[1,*]
[1]The Skaggs Institute for Chemical Biology and Departments of Chemistry and Immunology and the Worm Institute for Research and Medicine (WIRM), La Jolla, CA 92037, USA
[2]The Core Microscopy Facility, The Scripps Research Institute, 10550 North Torrey Pines Road, La Jolla, CA 92037, USA
[3]Computational Chemistry, Principia Biopharma, 400 East Jamie Court, South San Francisco, CA 94080, USA
*Correspondence: kdjanda@scripps.edu
http://dx.doi.org/10.1016/j.chembiol.2015.03.012

SUMMARY

The emergence of antibiotic resistance places a sense of urgency on the development of alternative antibacterial strategies, of which targeting virulence factors has been regarded as a "second generation" antibiotic approach. In the case of *Pseudomonas aeruginosa* infections, a proteolytic virulence factor, LasB, is one such target. Unfortunately, we and others have not been successful in translating in vitro potency of LasB inhibitors to in vivo efficacy in an animal model. To overcome this obstacle, we now integrate in silico and in vitro identification of the mercaptoacetamide motif as an effective class of LasB inhibitors with full in vivo characterization of mercaptoacetamide prodrugs using *Caenorhabditis elegans*. We show that one of our mercaptoacetamide prodrugs has a good selectivity profile and high in vivo efficacy, and confirm that LasB is a promising target for the treatment of bacterial infections. In addition, our work highlights that the *C. elegans* infection model is a user-friendly and cost-effective translational tool for the development of anti-virulence compounds.

INTRODUCTION

Pseudomonas aeruginosa is a nosocomial, opportunistic, Gram-negative bacteria causing various diseases including acute infections in immunocompromised patients and chronic lung infections in individuals with cystic fibrosis (Mesaros et al., 2007; Cohen and Prince, 2012). At the clinical level, *P. aeruginosa* is able to rapidly develop antibiotic resistance and form biofilms, thus it is extremely difficult to treat infected patients (Breidenstein et al., 2011). Moreover, *P. aeruginosa* infections are usually associated with a high morbidity and mortality rate ranging from 20% to 75%, despite improvements in hospital care. This undeniable medical challenge brings a sense of urgency to the development of alternative antibacterial strategies to currently available medications (El Solh and Alhajhusain, 2009; El-Solh et al., 2012).

The targeting of bacterial virulence factors as an effective means to control bacterial infections holds particular promise (Barczak and Hung, 2009; Clatworthy et al., 2007). Pathogenic bacteria produce virulence factors such as adhesion molecules, secretion systems, and other toxic factors including proteases to enhance their ability to cause disease and damage the host's tissues (Clatworthy et al., 2007). Indeed, *P. aeruginosa* pathogenesis presents itself through coordination of the expression of a plethora of virulence factors (Mesaros et al., 2007). Elastase B, also known as pseudolysin (LasB), is a zinc metalloprotease encoded by the *lasB* gene (Morihara et al., 1965). LasB has been shown to be highly toxic to the host through its enzymatic activity to degrade numerous components of innate and adaptive immune systems (Wretlind and Pavlovskis, 1983; Schultz and Miller, 1974; Mariencheck et al., 2003; Alcorn and Wright, 2004; Parmely et al., 1990). LasB can cause host tissue damage via hydrolysis of various components of the extracellular matrix and by breaching endothelial and epithelial barriers by attacking intercellular tight junctions (Azghani, 1996; de Bentzmann et al., 2000). Furthermore, proteomic analyses of laboratory and clinical *P. aeruginosa* strains have revealed that LasB production is increased in isolates from critically ill patients and ventilator-associated pneumoniae, and LasB activity is directly connected to the pro-inflammatory effects of *P. aeruginosa* infection (Le Berre et al., 2008; Bergamini et al., 2012). There are also reports of LasB being linked to *P. aeruginosa* biofilm formation and swarming (Tielen et al., 2010; Cathcart et al., 2011; Reimmann et al., 2002), suggesting a role in bacterial elution from the host's immune system.

Current animal models of *P. aeruginosa* infection include acute and chronic infections in mice and rats (Pavlovskis and Wretlind, 1979). Using these mammalian models, mitigation of bacterial virulence through disruption of LasB function has been demonstrated, suggesting that LasB is a promising therapeutic target (Kessler et al., 1983; Burns et al., 1990). Intriguing as the idea of virulence targeting is, a number of sobering fundamental challenges need to be addressed en route to the development of a viable LasB inhibitor. Foremost is that no LasB inhibitor has had its in vitro potency translate to in vivo efficacy in an animal model (Lewis, 2013). This discourse has led us to pursue a more practical non-mammalian animal model, *C. elegans*, for LasB inhibition optimization. Importantly, the strategies we disclose here for LasB in vivo targeting should be readily applicable to other bacterial virulence factors.

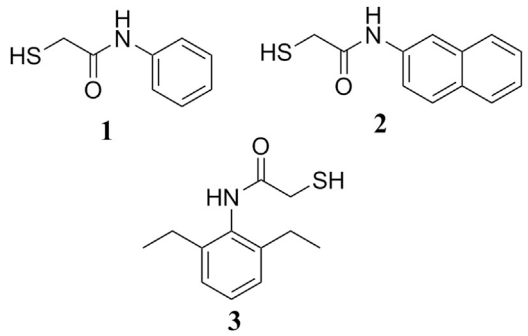

Figure 1. Hits Identified from In Silico and In Vitro Studies
Compounds identified from molecular docking studies and shown to inhibit LasB in vitro. Compounds **1**, **2**, and **3** possessed IC_{50} values of 156 ± 8, 27.4 ± 2.5, and 15.7 ± 3.1 μM, respectively.

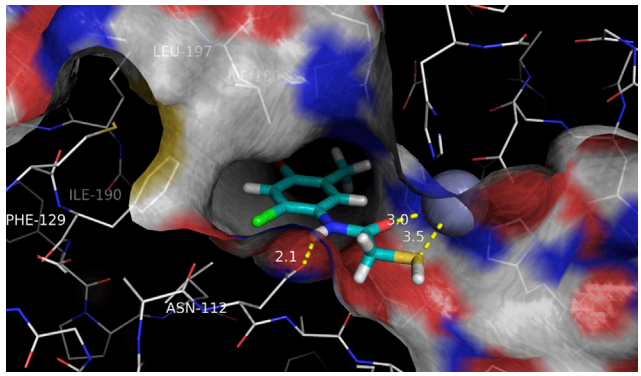

Figure 2. LasB Inhibitor Docked in the Active Site of Metalloproteinase
Compound **13** is shown docked using the Autocorrelator-derived model from the 3DBK structure. The docked orientation shows a close proximity between the thiol and zinc, a hydrogen bond between the amide of **13** and Asn112, and the phenyl ring shielding a collection of hydrophobic residues consisting of Phe129, Leu132, Val137, Ile190, and Leu197. Distance displayed in angstroms.

RESULTS

Virtual and In Vitro Screening against LasB

To initiate our screening efforts, virtual screening of all commercially available molecules from eMolecules containing a thiol appendage was performed. Restricting the search to molecules containing a thiol was done to increase the number of active molecules, as sulfur is known to act as a good ligand for zinc. To carry out the virtual screening, molecules were conformationally enumerated and docked using the defaults in Omega (v2.4.6. OpenEye Scientific Software; http://eyesopen.com) and Fred (v2.2.5 OpenEye Scientific Software; http://eyesopen.com), respectively (Hawkins et al., 2010; Hawkins and Nicholls, 2012; McGann, 2011). The ten highest scoring virtual candidates with a thiol within 5 Å from the catalytic zinc were selected for in vitro evaluation (Table S1).

The peptides found by Cathcart et al. (2011) were used to construct a model for potency with the Autocorrelator. This model was generated after the Autocorrelator used all available crystal structures of LasB, Omega (v2.4.6), and Fred (v2.2.5) to generate conformations. The Autocorrelator-derived model was then used as the basis for scaffold expansion experiments (see Supplemental Information) (Lardy et al., 2012).

This sub-library was screened using an in vitro LasB inhibition assay based on a LasB-cleavable fluorescence resonance energy transfer peptide substrate (see Supplemental Information) (Nishino and Powers, 1980). Of these compounds, three showed dose-dependent inhibition of LasB with half maximal inhibitory concentration (IC_{50}) values ranging from 15 to 160 μM (Figure 1). Interestingly, all active compounds (**1**, **2**, and **3**) contained an aromatic core with a mercaptoacetamide side chain, which suggests that this moiety plays an important role as a Zn^{2+} metal-binding chelator. We hypothesized that the thiol group and the electron-rich oxygen are critical for chelating the zinc atom of LasB, whereas the hydrophobic aromatic core fits in the ligand-binding cavity of the receptor pocket (Figure 2). Encouraged by our initial screening, a small series of compounds based on the active mercaptoacetamide motif were synthesized. These compounds contain a diverse array of substituents on the aromatic ring, including alkyl, halogens, ethers, and benzylamines. In addition, we varied the methylene chain length between the amide and thiol. The results from the LasB inhibition assay are summarized in Tables S2–S6.

Synthesis of Mercaptoacetamide Prodrugs

Following initial screening of our newly synthesized mercaptoacetamides, we successfully identified ten hits that demonstrated LasB antagonism (Table 1). Compounds **11**, **12**, and **13** were the most active with IC_{50} values ranging from 1.78 μM to 5.94 μM. We were excited by the potent in vitro activity of the hits identified, but it is well known that the thiol functionality is prone to oxidation in vivo. We sought to improve the stability of the compounds using a prodrug approach via acetylation of the thiol. As shown in Scheme S1, the commercially available aromatic amine was treated with chloroacetyl chloride to afford the α-chloro amide intermediate, which was then treated with potassium thioacetate to yield thioesters **11a**, **12a**, and **13a**. These prodrugs were subsequently hydrolyzed with potassium carbonate before performing the in vitro LasB inhibition assay.

Modulation of LasB Function in a *C. elegans* Infection Model

Having established several potent compounds that modulate LasB activity in vitro, we sought a simple animal model to provide us with a foundation for further development of these compounds in vivo. *C. elegans* has been increasingly used and studied for its potential as an intermediate model system for drug discovery between in vitro testing and a mammalian model (O'Reilly et al., 2014; Ewbank and Zugasti, 2011; Squiban and Kurz, 2011). *C. elegans* can succumb to human disease by simply feeding the worm with the respective pathogen, in converse worm infectivity can then be "cured" with common antibiotics at concentrations typically used to treat humans. Moreover, the *C. elegans* infection model has many practical advantages, such as being amenable to low-cost, large-scale in vivo screening and it does not raise any of the ethical concerns for drug testing at the early stages of development (Mahajan-Miklos

Table 1. Lead Mercaptoacetamides Identified In Vitro

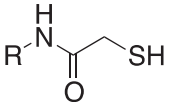

Compound	Structure	IC_{50} (μM)
4	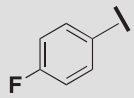	6.98 ± 0.07
5	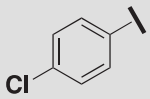	5.99 ± 0.11
6	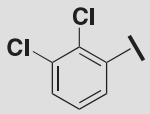	7.61 ± 0.03
7	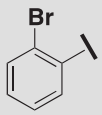	8.19 ± 0.22
8	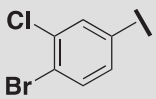	9.90 ± 0.09
9	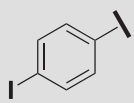	7.33 ± 0.02
10	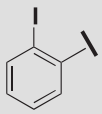	6.90 ± 0.01
11	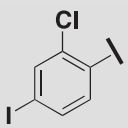	3.56 ± 0.04
12	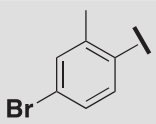	1.78 ± 0.01
13	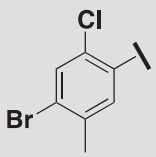	5.94 ± 0.02

et al., 1999; Tan et al., 1999a, 1999b; Kurz and Ewbank, 2000; Tan and Ausubel, 2000).

We first determined the effect of LasB on the ability of *P. aeruginosa* PAO1 to kill *C. elegans*, our reasoning here being that *C. elegans* has been used to compare the global variations of virulence in a *P. aeruginosa* "slow-killing" assay. In a typical *C. elegans* slow-killing assay, bacterial strains to be tested are used as a lawn on slow-killing agar plates, substituting in place of the normal feeding bacterium, *Escherichia coli* OP50. By simply ingesting pathogenic bacteria, worms can become infected, primarily in the intestine although exceptions have been observed (Dorer and Isberg, 2006). A comparison of median lethal time (LT_{50}) values in our present study confirmed that LasB activity significantly increased *P. aeruginosa*-induced virulence in a toxic infection compared with a genetic knockout ($\rho < 0.001$, Figure 3A). Our data indicate that when *C. elegans* is fed with wild-type PAO1, the worms survive up to 9 days with an LT_{50} of 3.9 ± 0.2 days, whereas the *lasB*-knockout-exposed animals survive up to 11 days with an LT_{50} of 6.5 ± 0.5 days. The extended lifespan observed in animals exposed to the *lasB* knockout provides strong evidence that using the *C. elegans* slow-killing assay is a valid model to evaluate LasB function in *P. aeruginosa* infections. Moreover, the assay can be used to quickly test and characterize the efficacy of in vitro LasB inhibitors in a whole-animal infection model.

With the *C. elegans* LasB assay at our beckoning, we next sought the importance of the inhibitors discovered in our in vitro assay. The most potent compounds (**11**, **12**, and **13**) and their corresponding thioester prodrugs (**11a**, **12a**, and **13a**, Table 2) were individually supplemented in slow-killing agar plates at 50 μM. Some of the administered compounds were able to modestly extend worm half-life, but none were as effective as **13a**. Mercaptoacetamide **13** demonstrated attenuation of *P. aeruginosa* virulence only at the early stages of infection with an LT_{50} of 4.3 ± 0.1 days. However, when **13** was masked as the thioacetate, **13a**, the half-life of the nematode was extended to 6.2 ± 0.1 days (Figure 3A). As observed in the supplemental bacterial cell viability minimum inhibitory concentration assay and mammalian cell cytotoxicity assay, **13** and **13a** had no effect on bacterial survival or mammalian cell viability at concentrations up to 50 μM, the highest concentration administered in the *C. elegans* slow-killing assay.

Accordingly, we further demonstrated that **13a** inhibited *P. aeruginosa* infection in *C. elegans* in a dose-dependent manner. At 25 μM, the LT_{50} of infected *C. elegans* was significantly increased to 1.5 days longer than that of wild-type PAO1 ($\rho < 0.001$, Figure 3B). However, when *C. elegans* was fed with wild-type PAO1 on plates supplemented at lower compound concentrations (5 and 10 μM), the virulence attenuation effect was diminished ($\Delta LT_{50} = 0.6$ days). Thus, **13a** provides a protective effect from the progression of *P. aeruginosa* infection in *C. elegans* through specific inhibition of LasB function.

Metalloenzyme Selectivity

Metalloproteins play an enormous role in modulating a wide array of functions in vivo, thus many laboratories are actively pursuing strategies that can modulate this class of proteins (Raeside and Strickland, 2012). At a clinical level, a contemporary goal of any successful therapeutic candidate is that it must possess

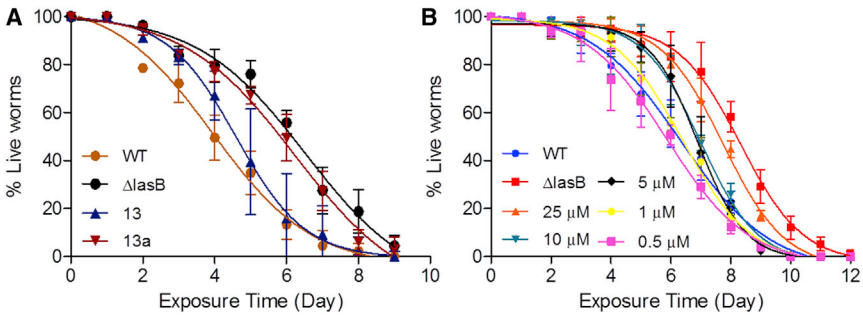

Figure 3. LasB Deletion and Treatment with 13a Extends *C. elegans* LT_{50} in a Dose-Dependent Manner

Survival rate of *P. aeruginosa*-infected *C. elegans* improves upon *lasB* deletion and supplementation of **13a** in the slow-killing assay.

(A) **13a** extends worm LT_{50} to 6.2 ± 0.1 days resulting in no significant difference between worm LT_{50} (6.5 ± 0.5 days) when fed *lasB* knockout *P. aeruginosa* ($\rho \geq 0.05$).

(B) Dose-dependent effect of **13a** on survival of *P. aeruginosa*-infected *C. elegans* over time in the slow-killing assay. *lasB* knockout (LT_{50} = 8.3 ± 0.1 days), 25 μM (LT_{50} = 7.8 ± 0.1 days), 10 μM (LT_{50} = 7.0 ± 0.1 days), 5 μM (LT_{50} = 7.0 ± 0.1 days), 1 μM (LT_{50} = 6.4 ± 0.1 days), 0.5 μM (LT_{50} = 5.9 ± 0.1 days), wild-type PAO1 (LT_{50} = 6.3 ± 0.2 days).

LT_{50} data were analyzed by ANOVA followed by Tukey's multiple comparison method to determine significance. Error bars represent SEM values (n = 3). WT, wild-type.

selectivity for the target of interest. Accordingly successful targeting of a singular metalloprotein appears chemically challenging, as it is estimated that approximately one third of all proteins are metalloproteins (Holm et al., 1996). Mercaptoacetamide **13** contains a metal-binding group that could incite promiscuity with other metalloproteases. To test this notion we screened **13** at 50, 25, and 12.5 μM against two ubiquitous metalloenzymes: matrix metalloproteinase 2 (MMP-2) and a Zn^{2+}-dependent histone deacetylase (HDAC, encompassing class I and IIb). MMP-2 is a Zn^{2+}-dependent endopeptidase that is capable of breaking down connective tissue including native and denatured collagens and elastin. Class I and IIb HDACs are known to regulate cellular processes via hydrolysis of the acetyl functionality embedded within protein matrices containing acetyl lysines. LasB and MMP-2 possess similar characteristics but HDAC operates under a different mechanism, thus inhibitor selectivity against these two enzymes would provide a measure of selectivity assurance. As shown in Figure 4, **13** did not inhibit enzyme activity of HDAC or MMP-2 at a dose range up to 50 μM.

Bioaccumulation and Metabolism of LasB Inhibitors in *C. elegans*

As an additional metric of the future potential of these mercaptoacetamides, we investigated their adsorption and metabolism in *C. elegans*. Accordingly, mercaptoacetamides **11**, **12**, and **13** and their respective prodrugs were examined as a means to correlate compound bioaccumulation with their bioactivity as seen in the slow-killing assays. Previous literature has documented how *C. elegans* could be resistant to a variety of pharmacological perturbations, so that the bioavailability of drug and drug metabolites in the worm is highly dependent on the drug's chemical structure and the drug delivery method (Zheng et al., 2013; Burns et al., 2010). Therefore, we used the same killing assay set up for the bioaccumulation test and collected the worms infected with *P. aeruginosa* 24 hr after seeding on the slow-killing assay plate supplemented with individual compounds. Collected worms were washed and homogenized for liquid chromatography-mass spectrometry (LC-MS) analysis, and the results are summarized in Table 2. In brief, mercaptoacetamides **11** and **11a** were not detected in the worm samples collected, indicating little or no accumulation of these two compounds. Mercaptoacetamides **12** and **12a** were also not identified in the worm homogenates, however, the disulfide form of **12** was observed in both samples. Interestingly, the metabolism of **13a** in *C. elegans* was more complex compared with **11a** and **12a**. The first stage of metabolism for **13a** was hydrolysis to generate the active thiol **13**, which was further oxidized to form the corresponding disulfide. Of the three thioacetates, only **13a** readily accumulated in *C. elegans* and metabolized to the active thiol form, and in so doing inhibited the function of LasB and extended the lifespan of *C. elegans*. It is noteworthy that these results match the bioactivity assay data as only **13a** significantly attenuated *P. aeruginosa* virulence in the slow-killing assay, providing support for our hypothesis that a prodrug strategy greatly improves the availability of active drug in the host organism.

Transmission Electron Microscopy

We used transmission electron microscopy (TEM) to visualize *P. aeruginosa* colonization, including virulence associated with LasB and its attenuation from **13a** treatment. Orchestrating this ensemble of events, we could examine the *C. elegans* intestine as a means to evaluate pathogenic progression at 48 hr post infection with/without LasB inhibitor treatment. Bacterial accumulation resulting in penetration of the intestinal lumen was classified as an unhealthy worm; worms without accumulation (and intact lumen) were classified as healthy. Using this outline to judge the infection rate, we scored worms based on frequency of encounter throughout the respective sample. Visualization of wild-type PAO1 infection indicated grossly distended intestinal lumen, widespread shortening of the microvilli, and direct contact of bacterial cells with the microvillar surface (Figure 5A). In 43% of cross sections (n = 7), we found bacterial cells that were not in the intestinal lumen (Figure 5B), indicating that *P. aeruginosa* cells had penetrated the intestinal wall and invaded other tissues.

In stark contrast with the *P. aeruginosa* wild-type, the *lasB* knockout exhibited lower levels of host tissue damage in *C. elegans* (Figure 5C). Analyzing cross sections, we encountered less than 20% (n = 10) of intracellular invasion and evaded bacterial cells in *lasB* mutant-infected animals compared with wild-type *P. aeruginosa*. Most promising was that in *C. elegans* treated with **13a**, less than 20% (n = 10) of the cross sections examined had tissue damage, which is comparable with the *lasB* mutant-infected worms, suggesting an alleviation in bacterial pathogenesis advancement (Figure 5D). As a control, we

Table 2. Characterization of Structural Metabolites from LasB Inhibitors in *C. elegans*

Compound	Parent Compound Identified	Identified Metabolites	Identified Metabolites
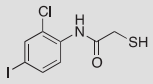 **11**	nd	nd	nd
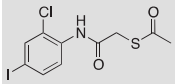 **11a**	nd	nd	nd
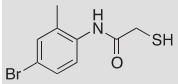 **12**	nd	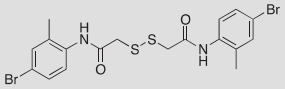	nd
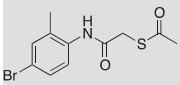 **12a**	nd	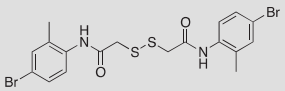	nd
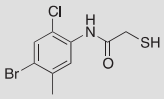 **13**	Yes	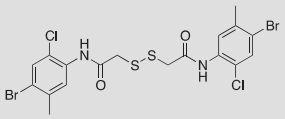	nd
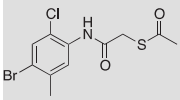 **13a**	Yes	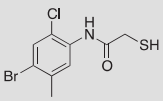	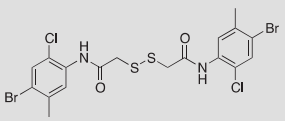

nd, none detected.

visualized worms fed with *E. coli* OP50 and observed normal intestinal lumina and microvilli structure (Figure S5). Complementing these findings, we also observed that lipid droplets filled in intestinal epithelial cells characterizing the intestine tissues from healthy worms (data not shown).

DISCUSSION

Developing a screening platform for antibiotic discovery that will eventually lead to molecules worthy of translational evaluation has been a challenge. At the clinical level, one must contend with the outbreak of resistant bacteria and diminishing returns from antibiotic research (Lewis, 2013). To address the increasing challenges in treating antibiotic-resistant bacterial infections, a range of alternative antibacterial strategies have been proposed. Of these tactics, investigation of virulence factors has been regarded as an emerging second generation antibiotic approach (Barczak and Hung, 2009; Clatworthy et al., 2007). The wisdom here is that virulence factors are not essential for cell viability, hence targeting such factors would impose weak or no selective pressure for the development and selection of drug resistance (Theuretzbacher, 2009). Arguably, it might be more prudent to inhibit transcription factors that control a number of virulence factors, rather than a single target. Taking this stance, LasR is a transcription factor found in *P. aeruginosa* and thought to be a major regulator of a plethora of virulence factors, including LasB (Kalia, 2013). Yet, strategically targeting LasR also has drawbacks as, under stress conditions, a signaling pathway termed IQS can supersede LasR and control a subset of quorum-controlled genes and thus proteins including LasB (Lee et al., 2013). Thus, efforts targeting LasR are highly valued; however, if *P. aeruginosa* engages the IQS circuitry, then inhibitors of LasR would not disengage LasB. At least for the case of LasB, we would argue that singular targeting of a virulence factor may be more effective.

A viable in vivo assay is especially crucial to overcome the substantial hurdles in bacterial drug development. Typically, cultured mammalian cells are used to simulate the potential host for bacterial infection. Using this approach, antibiotic efficiency and selectivity can be simultaneously determined by measuring the viability of bacterial and mammalian cells. However, targeting a virulence factor, in this case LasB, no significant

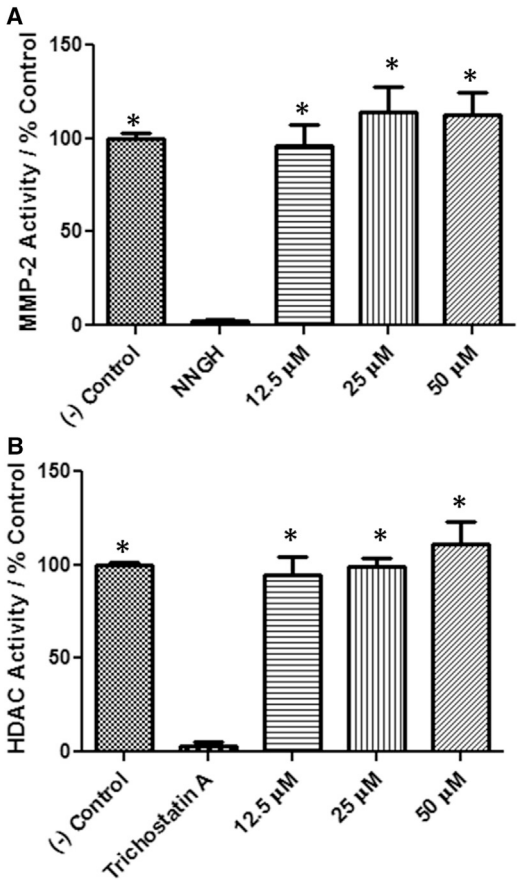

Figure 4. Selectivity of Compound 13 for LasB

Compound **13** was shown to be inactive against the metalloenzymes HDAC and MMP-2.

(A) MMP-2 retains activity in the presence of compound **13** (up to 50 μM). *N*-Isobutyl-*N*-(4-methoxyphenylsufonyl)-glycylhydroxamic acid (NNGH) is a known MMP-2 inhibitor and was used as a positive control.

(B) HDAC retains activity in the presence of compound **13** (up to 50 μM). Trichostatin A is a known HDAC inhibitor and was used as a positive control. Error bars represent SEM values ($n = 3$). Data were analyzed by ANOVA followed by Tukey's multiple comparison method to determine significance (*significantly different compared with the positive control, $\rho < 0.0001$).

bactericidal response is expected. Indeed, none of the mercaptoacetamides tested displayed toxicity toward *P. aeruginosa* or HeLa cells when tested at concentrations upward of 50 μM. Furthermore, the major host tissue damage caused by LasB is through the digestion of extracellular matrix proteins, rupturing cell connections, which renders the suitability of using a cultured single-cell mixture as an assay model ineffective. A whole-animal model such as the nematode *C. elegans* is multicellular with differentiated tissues and distinct organs, thus it is complex enough to address higher level biological questions while being simultaneously experimentally tractable. Using this enabled logic, we recapitulated LasB-induced pathogenesis in *C. elegans*, as shown in the nematode intestine TEM cross-section data and the extended worm lifespan with *lasB* mutant bacterial infection.

Our laboratory and others have reported several in vitro LasB inhibitors with micromolar IC_{50} values and nanomolar competitive inhibition constants (K_i) (Cathcart et al., 2011; Garner et al., 2012; Fullagar et al., 2013). Seeking to improve upon this research initiative, we used molecular docking to discover a mercaptoacetamide motif that inhibits the LasB protease. To improve upon inhibition, a series of molecules were prepared, which highlight how this scaffolding and its potency could be improved. Yet, a liability of the mercaptoacetamide motif is that it is prone to oxidation. Subsequently, we demonstrated how we could mask the thiol moiety as the thioacetate prodrug, which is ultimately hydrolyzed by xenobiotic esterases. Having established that *C. elegans* is a valuable disease model as defined by LasB, we examined how our small-molecule inhibitors of LasB would affect *P. aeruginosa* toxicity in *C. elegans*. Excitingly, **13** in its prodrug form was shown to be a highly efficient inhibitor of LasB function at the infection site, exhibiting the same level of virulence attenuation as the *lasB* mutant. Moreover, **13** presented a selectivity measure as shown by the lack of inhibitory activity observed against HDAC and MMP-2.

As a means to correlate our in vitro and in vivo data, we studied the metabolism and bioaccumulation of selected LasB inhibitors. Worm lysate was extracted, separated, and visualized by LC-MS to analyze compound accumulation and metabolism in the worm, partially mimicking ADME (absorption, distribution, metabolism, and excretion) studies in animal models. Mercaptoacetamide **13**, as anticipated, was oxidized thus abrogating in vivo efficacy. However, when **13** was masked in the form of a prodrug, **13a**, we observed the release of the active compound in the host organism and thus extended worm LT_{50}. When masked as prodrugs the other mercaptoacetamides, **11** and **12** showed minimal effect on alleviating bacterial virulence and were either not detected or observed only in the inactive disulfide form. Presumably, these mercaptoacetamides have different molecular interactions with the esterases in *C. elegans*, which results in different metabolism profiles of these three compounds. In total, the highly correlated data between IC_{50}, LT_{50}, TEM, and bioaccumulation substantiate the pertinence of a worm-based in vivo model system.

In summary, through a virtual screening effort we discovered a core unit (the mercaptoacetamides) that could inhibit the metalloprotease LasB at a non-toxic concentration. Focusing upon this architecture, a series of molecules were prepared, three of which potently disabled the protease. The mercaptoacetamides discovered, while excellent in vitro inhibitors, possessed a serious liability, a thiol capable of being oxidized. We were thus led to ask whether a prodrug approach might serve as a better in vivo surrogate. Using a prodrug approach to mask the reactive thiol, we were successful in translating an initial in vitro lead into a more drug-like molecule with in vivo efficacy. We have established how *C. elegans* can be used to understand the impact of a bacterial virulence factor and how host-pathogen interactions between *C. elegans* and *P. aeruginosa* readily model the disease state seen in mammalian models. Importantly, this *C. elegans* animal infection model has allowed us to systematically investigate the bioaccumulation of metabolites from an active compound, thus showing that this model can be used to study how compounds are metabolized in vivo. It is interesting to note that compounds that did not translate into in vivo efficacy did not accumulate in the nematode. From a medicinal chemistry prospective, this study opens new avenues for the rapid

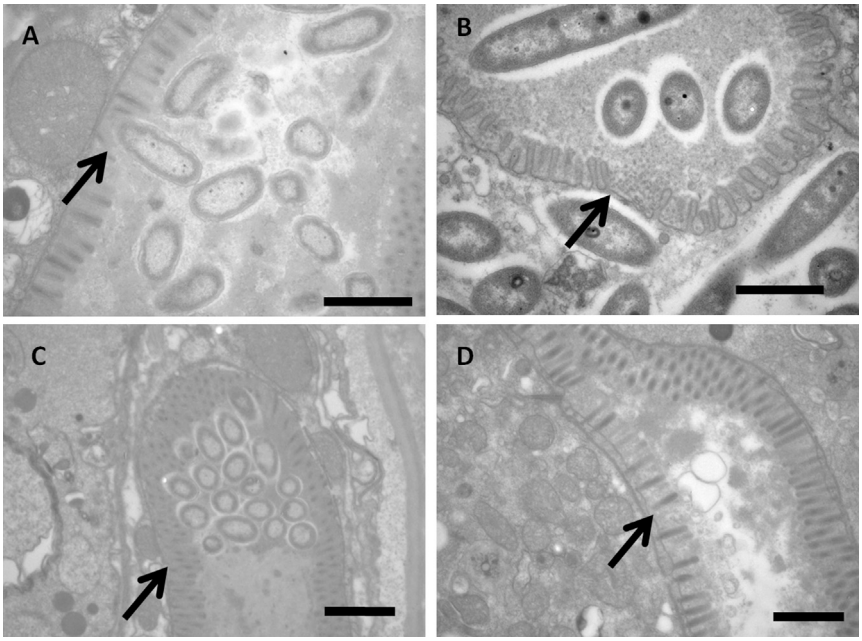

Figure 5. *C. elegans* Intestine Cross Sections as Viewed by Transmission Electron Microscopy

Cross sections of bacterial accumulation in *C. elegans* intestine used for invasion frequency experiments.

(A) Worms fed with PAO1 demonstrate bacterial cell accumulation in the lumen and shortened microvilli due to bacterial penetration.

(B) Worms fed with PAO1 have punctured intestinal walls.

(C) Worms fed with *lasB* knockout have normal intestinal structure.

(D) Image of PAO1-fed worm treated with **13a**, showing intact intestinal lumen and reversal of bacterial pathogenesis. Arrows indicate the object of relevance. Scale bar represents 1 μm.

development of novel anti-infective strategies that target specific virulence mechanisms.

SIGNIFICANCE

Utilizing a *lasB* genetic knockout, the relevance of this virulence factor in a *P. aeruginosa* infection model of the nematode *C. elegans* was validated. Molecular docking studies led to the discovery of the mercaptoacetamide class of non-peptidic small-molecule inhibitors of LasB. We were able to show that *C. elegans* is an excellent translational tool for the medicinal chemist seeking to develop anti-virulence compounds, as an in vitro lead was shown to have in vivo activity. Also marshaled through this research was that compound bioaccumulation and metabolism could be readily assessed in a user-friendly animal model. Indeed, this infection model enables the screening of anti-virulence compounds at minimal cost compared with its expensive mammalian counterparts. Lastly, we were able to visualize the immediate anti-virulence restorative effect of a LasB inhibitor using electron microscopy, as the phenotype mirrored that of the *lasB* knockout strain. Importantly, our studies provide not only tools to expand our understanding of the relevance of bacterial metalloproteases in *P. aeruginosa* pathogenesis but also the first steps toward a contemporary goal of validating proteolytic virulence factors, including LasB, as new therapeutic targets for the development of effective treatments for bacterial infections.

EXPERIMENTAL PROCEDURES

In Vitro Fluorescence Assay for LasB Activity

LasB was purchased from Elastin Products Company and used as received. The LasB pro-fluorescent substrate, Abz-Ala-Gly-Leu-Ala-*p*-nitro-benzyl-amide (SAG-3905-PI), was purchased from Peptides International and used as received. An in vitro fluorescence-based peptide cleavage assay was adapted from a previously reported assay and performed in 96-well microtiter plates (Corning Costar, black with clear bottom). Assays were performed in 100 μl of assay buffer (50 mM Tris-HCl, 2.5 mM $CaCl_2$, 1% dimethylformamide [pH 7]) containing 2 mg/ml LasB, 250 μM Abz-Ala-Gly-Leu-Ala-*p*-nitro-benzyl-amide substrate, and varying concentration of inhibitors. The reaction system was pre-incubated at 37°C for 30 min before the addition of peptide substrates and monitored by measuring the increase in fluorescence for 30 min (λ_{ex} = 340 nm, λ_{em} = 415 nm) at 37°C on a SpectraMax M2^e microplate reader (Molecular Devices). LasB activity was evaluated by the slope during the linear phase of the cleavage as units of fluorescence per unit time. The activities obtained at different compound concentrations were analyzed by GraphPad Prism 5 to afford the IC_{50} values for each inhibitor identified.

In Vitro Fluorescence Assay for HDAC and MMP-2 Activity

A Fluorogenic HDAC Assay Kit (Green) was purchased from BPS Bioscience and used according to the manufacturer's instructions. The MMP-2 Fluorometric Drug Discovery Kit was purchased from Enzo Life Sciences and used according to the manufacturer's instructions, with a slight modification as described previously (Day and Cohen, 2013). Following inhibitor and enzyme incubation (37°C for 30 min), the substrate was added to initiate the reaction. The change in fluorescence (λ_{ex} = 305 nm, λ_{em} = 405 nm) was monitored for 30 min on a SpectraMax M2^e microplate reader (Molecular Devices). Control wells containing enzyme and substrate (no inhibitor) were designated as negative controls wells. The increase in fluorescence in the inhibitor wells was compared with that in the negative control wells and is presented as a percentage. The negative control wells were set to 100% enzyme activity and inhibitor wells were normalized against this value. All assays were performed in triplicate.

C. elegans Slow-Killing Assays

C. elegans slow-killing assays were performed following a previous protocol with minor modifications. The wild-type *C. elegans* (Bristol) N2 hermaphrodite strain was used in the slow-killing assays. Worms were synchronized by hypochlorite treatment of gravid adults. Synchronized worms were grown to L4 or young adult stage by incubating them at 25°C in Nematode Growth Medium (NGM) as stock for the killing assays. 3.5-cm slow-killing agar plates were made following the published recipe with the addition of 0.3% DMSO or the designated testing compounds at 50 μM. One-day-old agar plates were inoculated with 10 μl of an overnight culture in lysogeny broth medium of *P. aeruginosa* PAO1 or *lasB* knockout (*lasB*$^-$) or *E. coli* OP50 and incubated at 37°C for 24 hr and at 25°C for another 24–48 hr to form a lawn of bacteria. Nematodes were washed off the stock plates and suspended in a minimal volume of M9 buffer (pH 6.5). 20–30 L4 stage or adult hermaphrodite worms were placed on each slow-killing plate for evaluation of bacterial infection. Plates were incubated at 25°C and scored for live worms every 24 hr. A worm was considered dead when it no longer responded to touch when picked up by a

sterile platinum wire loop. Killing curves represent the mean of three separate replicate plates per condition.

C. elegans Bioaccumulation Assays

Sample preparation and analysis of worm homogenates were carried out as reported previously (Gooyit et al., 2014). Mass spectrometry acquisition was performed in negative electrospray ionization mode with the following parameters: capillary voltage = 3.5 kV, nebulizer pressure = 20 psig, drying gas flow = 7 l/min, and gas temperature = 350°C. Worm homogenate samples were analyzed on a Zorbax SB-C18 column (3.5 μm, 1 × 150 mm; Agilent Technologies). The mobile phase consisted of elution at 0.10 ml/min starting with 70% A/30% B for 1 min, followed by a 5-min linear gradient to 100% B, and then 100% B for 12 min. The mass filters used for extracting ion chromatograms were as follows: *m/z* = 333.910–333.950 for **13a**, *m/z* = 291.900–291.940 for **13**, *m/z* = 584.780–584.850 for the disulfide of **13**, *m/z* = 299.700–300.100 for **11a**, *m/z* = 257.900–258.100 for **11**, *m/z* = 516.700–517.100 for the disulfide form of **11**, *m/z* = 367.600–368.200 for **12a**, *m/z* = 325.600–326.100 for **12**, *m/z* = 650.400–651.000 for the disulfide form **12**. Identification of compounds in the worm homogenates was confirmed by comparison of high-pressure liquid chromatography retention time and mass spectrum with those of authentic synthetic standards (Figure S4).

Electron Microscopy

C. elegans infection sample preparation for electron microscopy was the same as described for the slow-killing assay. After 48 hr incubation at 25°C, animals were collected and incubated in fixation buffer (2.5% glutaraldehyde, 1.0% paraformaldehyde in 0.05 M sodium cacodylate buffer (pH 7.4) plus 3.0% sucrose). During the initiation of fixation, animals were cut in half with a surgical blade in a drop of fixative under a dissecting microscope, fixed overnight at 4°C, rinsed in 0.1 M cacodylate buffer, post-fixed in 1.0% osmium tetroxide 0.1 M cacodylate buffer, rinsed in buffer and water, and stained en bloc in 2% aqueous uranyl acetate. After rinsing in water, animals were embedded in 2% agarose in PBS, dehydrated through a graded series of ethanol washes to 100%, then 100% propylene oxide, and finally 1:1 propylene oxide/EPON overnight. Blocks were infiltrated in 100% EPON and then embedded in fresh EPON overnight at 60°C. Thin sections were cut on a Reichert Ultracut E ultramicrotome and collected on formvar-coated gold grids. Sections were post-stained with uranyl acetate and lead citrate and viewed using a JEOL 1011 transmission electron microscope at 80 kV with an AMT digital imaging system (Advanced Microscopy Techniques). For each observation, whenever possible at least ten cross sections were evaluated and representative images were chosen.

Computational Methodology

Three different structures of LasB (PDB codes 3DBK, 1EZM, 1U4G) were used in Autocorrelator runs to construct computational models of potency against LasB (Lardy et al., 2012). While all three structures are reasonably similar, with subtle differences between them in the catalytic cleft, there was a preference by the Autocorrelator for the 3DBK structure. The correlation coefficients (R2) for the strongest models built with 3DBK, 1EZM, and 1U4G were 0.61, 0.49, and 0.47, respectively.

The model found with the 3DBK structure of LasB employed Omega 2.4.6 (using a maximum of 280 conformations per molecule and a 10-kcal energy window cutoff) and Fred 2.2.5 (with the chemscore scoring function, shapegauss optimization, no MMFF (Merck molecular force fields) refinement, 16.0 Å added to the bounding box containing the co-crystalized inhibitor, a clash_scale of 0.8, a low contour quality, rotational and translational step size of 1.2, and chemgauss 2 for exhaustive scoring) (Hawkins et al., 2010; Hawkins and Nicholls, 2012; McGann, 2011). The Autocorrelator turns off all the pose_select options in Fred by default. The scoring function produced from the LARS methodology in R contains terms for the metal interaction, hydrophobic interactions, and rotatable bonds (McGann et al., 2003; Efron et al., 2004). The scoring function is shown in Equation 1:

$$\text{predIC}_{50} = 2.84 + \text{Chemscore.RB} \times 0.36 + \text{Chemscore.LIPO} \times -0.115 + \text{Chemscore.METAL} \times 0.0785, \quad \text{(Equation 1)}$$

A total of 39,816 thiol-containing purchasable molecules were virtually screened by this method and were ranked using Equation 1.

SUPPLEMENTAL INFORMATION

Supplemental Information includes Supplemental Methods and Materials, five figures, one scheme, and six tables and can be found with this article online at http://dx.doi.org/10.1016/j.chembiol.2015.03.012.

ACKNOWLEDGMENTS

We would like to thank Dr. Michael Petrascheck for generously donating the microscope used for the studies described in this article. We thank Dr. Kirthi Reddy, Dr. Kendra Rumbaugh, and Emily Troemel for providing the *P. aeruginosa* strains and insightful discussion regarding the experimental protocol. We appreciate advice from Dr. Gunnar Kaufmann throughout this project, and we would also like to thank Paul Bremer for helping with the molecular docking studies. We would also like to acknowledge OpenEye Scientific Software for the use of their software through their free academic licensing program. The work was supported by Skaggs Institute for Chemical Biology.

Received: January 14, 2015
Revised: February 18, 2015
Accepted: March 2, 2015
Published: April 16, 2015

REFERENCES

Alcorn, J.F., and Wright, J.R. (2004). Degradation of pulmonary surfactant protein D by *Pseudomonas aeruginosa* elastase abrogates innate immune function. J. Biol. Chem. *279*, 30871–30879.

Azghani, A.O. (1996). *Pseudomonas aeruginosa* and epithelial permeability: role of virulence factors elastase and exotoxin A. Am. J. Respir. Cell Mol. Biol. *15*, 132–140.

Barczak, A.K., and Hung, D.T. (2009). Productive steps toward an antimicrobial targeting virulence. Curr. Opin. Microbiol. *12*, 490–496.

Bergamini, G., Di Silvestre, D., Mauri, P., Cigana, C., Bragonzi, A., De Palma, A., Benazzi, L., Döring, G., Assael, B.M., Melotti, P., et al. (2012). MudPIT analysis of released proteins in *Pseudomonas aeruginosa* laboratory and clinical strains in relation to pro-inflammatory effects. Integr. Biol. *4*, 270–279.

Breidenstein, E.B., de la Fuente-Nunez, C., and Hancock, R.E. (2011). *Pseudomonas aeruginosa*: all roads lead to resistance. Trends Microbiol. *19*, 419–426.

Burns, F.R., Paterson, C.A., Gray, R.D., and Wells, J.T. (1990). Inhibition of *Pseudomonas aeruginosa* elastase and *Pseudomonas keratitis* using a thiol-based peptide. Antimicrob. Agents Chemother. *34*, 2065–2069.

Burns, A.R., Wallace, I.M., Wildenhain, J., Tyers, M., Giaever, G., Bader, G.D., Nislow, C., Cutler, S.R., and Roy, P.J. (2010). A predictive model for drug bioaccumulation and bioactivity in *Caenorhabditis elegans*. Nat. Chem. Biol. *6*, 549–557.

Cathcart, G.R., Quinn, D., Greer, B., Harriott, P., Lynas, J.F., Gilmore, B.F., and Walker, B. (2011). Novel inhibitors of the *Pseudomonas aeruginosa* virulence factor LasB: a potential therapeutic approach for the attenuation of virulence mechanisms in pseudomonal infection. Antimicrob. Agents Chemother. *55*, 2670–2678.

Clatworthy, A.E., Pierson, E., and Hung, D.T. (2007). Targeting virulence: a new paradigm for antimicrobial therapy. Nat. Chem. Biol. *3*, 541–548.

Cohen, T.S., and Prince, A. (2012). Cystic fibrosis: a mucosal immunodeficiency syndrome. Nat. Med. *18*, 509–519.

Day, J.A., and Cohen, S.M. (2013). Investigating the selectivity of metalloenzyme inhibitors. J. Med. Chem. *56*, 7997–8007.

de Bentzmann, S., Polette, M., Zahm, J.M., Hinnrasky, J., Kileztky, C., Bajolet, O., Klossek, J.M., Filloux, A., Lazdunski, A., Puchelle, E., et al. (2000). *Pseudomonas aeruginosa* virulence factors delay airway epithelial wound repair by altering the actin cytoskeleton and inducing overactivation of epithelial matrix metalloproteinase-2. Lab. Invest. *80*, 209–219.

Dorer, M.S., and Isberg, R.R. (2006). Non-vertebrate hosts in the analysis of host-pathogen interactions. Microbes Infect. *8*, 1637–1646.

 ©2015 Elsevier Ltd All rights reserved

Efron, B., Hastie, T., Johnstone, I., and Tibshirani, R. (2004). Least angle regression. Ann. Stat. *32*, 407–499.

El Solh, A.A., and Alhajhusain, A. (2009). Update on the treatment of *Pseudomonas aeruginosa* pneumonia. J. Antimicrob. Chemother. *64*, 229–238.

El-Solh, A.A., Hattemer, A., Hauser, A.R., Alhajhusain, A., and Vora, H. (2012). Clinical outcomes of type III *Pseudomonas aeruginosa* bacteremia. Crit. Care Med. *40*, 1157–1163.

Ewbank, J.J., and Zugasti, O. (2011). C. elegans: model host and tool for antimicrobial drug discovery. Dis. Model. Mech. *4*, 300–304.

Fullagar, J.L., Garner, A.L., Struss, A.K., Day, J.A., Martin, D.P., Yu, J., Cai, X., Janda, K.D., and Cohen, S.M. (2013). Antagonism of a zinc metalloprotease using a unique metal-chelating scaffold: tropolones as inhibitors of *P. aeruginosa* elastase. Chem. Commun. (Camb.) *49*, 3197–3199.

Garner, A.L., Struss, A.K., Fullagar, J.L., Agrawal, A., Moreno, A.Y., Cohen, S.M., and Janda, K.D. (2012). 3-Hydroxy-1-alkyl-2-methylpyridine-4(1H)-thiones: inhibition of the *Pseudomonas aeruginosa* virulence factor LasB. ACS Med. Chem. Lett. *3*, 668–672.

Gooyit, M., Tricoche, N., Lustigman, S., and Janda, K.D. (2014). Dual protonophore–chitinase inhibitors dramatically affect *O. volvulus* molting. J. Med. Chem. *57*, 5792–5799.

Hawkins, P.C.D., and Nicholls, A. (2012). Conformer generation with OMEGA: learning from the data set and the analysis of failures. J. Chem. Inf. Model. *52*, 2919–2936.

Hawkins, P.C.D., Skillman, A.G., Warren, G.L., Ellingson, B.A., and Stahl, M.T. (2010). Conformer generation with OMEGA: algorithm and validation using high quality structures from the Protein Databank and Cambridge Structural Database. J. Chem. Inf. Model. *50*, 572–584.

Holm, R.H., Kennepohl, P., and Solomon, E.I. (1996). Structural and functional aspects of metal sites in biology. Chem. Rev. *96*, 2239–2314.

Kalia, V.C. (2013). Quorum sensing inhibitors: an overview. Biotechnol. Adv. *31*, 224–245.

Kessler, E., Spierer, A., and Blumberg, S. (1983). Specific inhibition of *Pseudomonas aeruginosa* elastase injected intracorneally in rabbit eyes. Invest. Ophthalmol. Vis. Sci. *24*, 1093–1097.

Kurz, C.L., and Ewbank, J.J. (2000). *Caenorhabditis elegans* for the study of host-pathogen interactions. Trends Microbiol. *8*, 142–144.

Lardy, M.A., LeBrun, L., Bullard, D., Kissinger, C., and Gobbi, A. (2012). Building a three-dimensional model of CYP2C9 inhibition using the Autocorrelator: an autonomous model generator. J. Chem. Inf. Model. *52*, 1328–1336.

Le Berre, R., Nguyen, S., Nowak, E., Kipnis, E., Pierre, M., Ader, F., Courcol, R., Guery, B.P., and Faure, K. (2008). Quorum-sensing activity and related virulence factor expression in clinically pathogenic isolates of *Pseudomonas aeruginosa*. Clin. Microbiol. Infect. *14*, 337–343.

Lee, J., Wu, J., Deng, Y., Wang, J., Wang, C., Wang, J., Chang, C., Dong, Y., Williams, P., and Zhang, L.H. (2013). A cell-cell communication signal integrates quorum sensing and stress response. Nat. Chem. Biol. *9*, 339–343.

Lewis, K. (2013). Platforms for antibiotic discovery. Nat. Rev. Drug Discov. *12*, 371–387.

Mahajan-Miklos, S., Tan, M.W., Rahme, L.G., and Ausubel, F.M. (1999). Molecular mechanisms of bacterial virulence elucidated using a *Pseudomonas aeruginosa-Caenorhabditis elegans* pathogenesis model. Cell *96*, 47–56.

Mariencheck, W.I., Alcorn, J.F., Palmer, S.M., and Wright, J.R. (2003). *Pseudomonas aeruginosa* elastase degrades surfactant proteins A and D. Am. J. Respir. Cell Mol. Biol. *28*, 528–537.

McGann, M. (2011). FRED pose prediction and virtual screening accuracy. J. Chem. Inf. Model. *51*, 578–596.

McGann, M.R., Almond, H.R., Nicholls, A., Grant, J.A., and Brown, F.K. (2003). Gaussian docking functions. Biopolymers *68*, 76–90.

Mesaros, N., Nordmann, P., Plésiat, P., Roussel-Delvallez, M., Van Eldere, J., Glupczynski, Y., Van Laethem, Y., Jacobs, F., Lebecque, P., Malfroot, A., et al. (2007). *Pseudomonas aeruginosa*: resistance and therapeutic options at the turn of the new millennium. Clin. Microbiol. Infect. *13*, 560–578.

Morihara, K., Tsuzuki, H., Oka, T., Inoue, H., and Ebata, M. (1965). *Pseudomonas aeruginosa* elastase isolation, crystallization, and preliminary characterization. J. Biol. Chem. *240*, 3295–3304.

Nishino, N., and Powers, J.C. (1980). *Pseudomonas aeruginosa* elastase. Development of a new substrate, inhibitors, and an affinity ligand. J. Biol. Chem. *255*, 3482–3486.

O'Reilly, L.P., Luke, C.J., Perlmutter, D.H., Silverman, G.A., and Pak, S.C. (2014). *C. elegans* in high-throughput drug discovery. Adv. Drug Deliv. Rev. *69-70*, 247–253.

Parmely, M., Gale, A., Clabaugh, M., Horvat, R., and Zhou, W.W. (1990). Proteolytic inactivation of cytokines by *Pseudomonas aeruginosa*. Infect. Immun. *58*, 3009–3014.

Pavlovskis, O.R., and Wretlind, B. (1979). Assessment of protease (elastase) as a *Pseudomonas aeruginosa* virulence factor in experimental mouse burn infection. Infect. Immun. *24*, 181–187.

Raeside, A., and Strickland, I. (2012). World Preview 2018: Embracing the Patent Cliff. (EvaluatePharma).

Reimmann, C., Ginet, N., Michel, L., Keel, C., Michaux, P., Krishnapillai, V., Zala, M., Heurlier, K., Triandafillu, K., Harms, H., et al. (2002). Genetically programmed autoinducer destruction reduces virulence gene expression and swarming motility in *Pseudomonas aeruginosa* PAO1. Microbiology *148*, 923–932.

Schultz, D.R., and Miller, K.D. (1974). Elastase of *Pseudomonas aeruginosa*: inactivation of complement components and complement-derived chemotactic and phagocytic factors. Infect. Immun. *10*, 128–135.

Squiban, B., and Kurz, C.L. (2011). *C. elegans*: an all in one model for antimicrobial drug discovery. Curr. Drug Targets *12*, 967–977.

Tan, M.W., and Ausubel, F.M. (2000). *Caenorhabditis elegans*: a model genetic host to study *Pseudomonas aeruginosa* pathogenesis. Curr. Opin. Microbiol. *3*, 29–34.

Tan, M.W., Mahajan-Miklos, S., and Ausubel, F.M. (1999a). Killing of *Caenorhabditis elegans* by *Pseudomonas aeruginosa* used to model mammalian bacterial pathogenesis. Proc. Natl. Acad. Sci. USA *96*, 715–720.

Tan, M.W., Rahme, L.G., Sternberg, J.A., Tompkins, R.G., and Ausubel, F.M. (1999b). *Pseudomonas aeruginosa* killing of *Caenorhabditis elegans* used to identify *P. aeruginosa* virulence factors. Proc. Natl. Acad. Sci. USA *96*, 2408–2413.

Theuretzbacher, U. (2009). Antibiotics: derivative drugs, novel compounds and the need for effective resistance strategies. Future Microbiol. *4*, 1243–1247.

Tielen, P., Rosenau, F., Wilhelm, S., Jaeger, K.E., Flemming, H.C., and Wingender, J. (2010). Extracellular enzymes affect biofilm formation of mucoid *Pseudomonas aeruginosa*. Microbiology *156*, 2239–2252.

Wretlind, B., and Pavlovskis, O.R. (1983). *Pseudomonas aeruginosa* elastase and its role in pseudomonas infections. Rev. Infect. Dis. *5*, S998–S1004.

Zheng, S.Q., Ding, A.J., Li, G.P., Wu, G.S., and Luo, H.R. (2013). Drug absorption efficiency in *Caenorhbditis elegans* delivered by different methods. PLoS One *8*, e56877.